Hindawi Publishing Corporation
Journal of Catalysts
Volume 2014, Article ID 370696, 7 pages
http://dx.doi.org/10.1155/2014/370696

Research Article

Synthesis of V_2O_5 Nanoflakes on PET Fiber as Visible-Light-Driven Photocatalysts for Degradation of RhB Dye

Yim-Leng Chan, Swee-Yong Pung, and Srimala Sreekantan

Science and Engineering of Nanomaterials Team, School of Materials and Mineral Resources Engineering, Universiti Sains Malaysia, Engineering Campus, Seri Ampangan, 14300 Nibong Tebal, Pulau Pinang, Malaysia

Correspondence should be addressed to Swee-Yong Pung; sypung@usm.my

Received 26 May 2014; Revised 27 July 2014; Accepted 28 July 2014; Published 17 August 2014

Academic Editor: Adel A. Ismail

Copyright © 2014 Yim-Leng Chan et al. This is an open access article distributed under the Creative Commons Attribution License, which permits unrestricted use, distribution, and reproduction in any medium, provided the original work is properly cited.

The visible-light-driven semiconductor photocatalysts are the current research focus techniques used to decompose organic pollutants/compounds. The photodegradation efficiency of organic compounds by photocatalyst is expected to be better compared to UV-light-driven semiconductor photocatalysts technique since the major components of our solar energy are visible light (~44%). However, as most of the previous research work has been carried out using semiconductor photocatalysts in the form of powder, extra steps and costs are needed to remove this powder from the slurry to prevent secondary pollution. In this research work, we will explain our fabrication technique of V_2O_5 nanoflakes by growing radially on PET fibers. By utilizing the flexibility and high surface area of polymeric fibers as novel substrate for the growth of V_2O_5 nanoflakes, the Rhodamine B (RhB) could be degraded under visible light irradiation. The photodegradation of RhB solution by V_2O_5 nanoflakes followed the 1st order kinetic with a constant rate of 0.0065 min^{-1}. The success of this research work indicates that V_2O_5 nanoflakes grown on PET fibre could be possibly used as organic waste water purifier under continuous flow condition. A photodegradation mechanism of V_2O_5 nanostructures to degrade RhB dye is proposed based on the energy diagram.

1. Introduction

Water pollution is one of the most serious environmental problems. Many untreated organic effluents such as dyes from textile industries are being discharged into the ecosystem, creating severe environmental pollution by releasing toxic and potential carcinogenic substances into the environment [1]. Therefore, various wastewater treatment processes such as precipitation, adsorption by activated carbon, coagulation, and membrane ultrafiltration have been developed for the removal of these organic pollutants [2–5]. However, these wastewater treatment processes are simply transforming the pollutants from one phase to another, leading to secondary pollution problems.

Recently, there has been a growing interest in the utilization of advanced oxidation processes (AOPs) via semiconductor photocatalysts for the organic pollutants removal. In AOPs, highly reactive species such as hydroxyl radicals are generated to oxidize a broad range of organic pollutants rapidly and nonselectively. Semiconductor photocatalysts are widely used due to their unique strengths for complete mineralization of organic pollutants into less harmful byproduct such as water, CO_2, and mineral acids. For example, zinc oxide (ZnO) nanoparticles [6–10] and titanium oxide (TiO_2) nanoparticles [11–13] were frequently used by researchers as UV-driven photocatalysts to decompose organic compounds/pollutants because of their wide band gap.

Development of visible-light-driven semiconductor photocatalysts for organic compounds removal is our current research focus. This is because the visible light accounts for 45% of the total energy of solar spectrum, while UV light only represents less than 10%. Theoretically, the photodegradation efficiency of organic compounds by semiconductor photocatalysts in visible light irradiation could be further enhanced. Several methods have been explored to develop visible-light-driven semiconductor photocatalysts. This could be done by shifting the band gap absorption edge of wide band gap semiconductors to a longer wavelength via metal or nonmetal doping. For example, Cu doped ZnO nanorods [14] and Cd doped ZnO nanostructures [15] responded to visible light

irradiation in degradation of organic dyes. Furthermore, narrow band gap semiconductor such as manganese oxide (MnO_2) nanoparticles [16, 17] and vanadium dioxide (VO_2) nanoparticles [18] could also be used as visible-light-driven photocatalysts. Normally, H_2O_2 chemical was required to improve the photodegradation efficiency of these semiconductor photocatalysts in degradation of organic compounds under visible light irradiation [19].

Regardless of UV- or visible-light-driven photocatalysts, most of the previous research used semiconductor in the form of nanoparticles for organic compounds removal. This is because semiconductor nanoparticles collectively have a high surface area, resulting in effective generation of free radicals and decomposition of organic compounds. The limitation of using semiconductor nanoparticles is that there is a need for the removal of nanoparticles from the slurry via centrifugation [20]. This addition step is time consuming and adds extra cost to the overall process. This additional processing step for the removal of semiconductor nanoparticles can be avoided by growing semiconductor nanostructures rigid substrates such as stainless steel wire [21].

In this work, vanadium pentoxide (V_2O_5) was selected as visible-light-driven semiconductor to be grown on flexible substrate, that is, polyethylene terephthalate (PET) fibre attributed to its narrow band gap (2.52 eV). There are various synthesis methods that could be used to produce the V_2O_5 nanostructures and thin films. For instances, Wei and Zhang synthesized V_2O_5 nanotubes using hydrothermal method [22] and Yin et al. grew porous V_2O_5 micro/nanotubes by chemical vapor deposition [23]. In addition, Blanquart et al. deposited V_2O_5 thin films using atomic layer deposition [24] and Gotić et al. synthesized V_2O_5 powder by sol-gel method [25]. As the V_2O_5 nanoflakes were to be grown on PET fibre, sol-gel method was chosen because of its low synthesis temperature (<100°C) and possibility of upscaling the synthesis process.

The synthesis condition of V_2O_5 nanoparticles using sol-gel method was first established. Subsequently, this synthesis condition was applied to synthesize V_2O_5 nanoflakes on PET fibre. The PET fibre offers more flexibility in handling as compared to stainless steel wire during setting up organic waste purifier. The photocatalytic activities of both V_2O_5 nanoparticles and V_2O_5 nanoflakes which have grown on PET fibre in degradation of RhB dye ($C_{28}H_{31}ClN_2O_3$) under visible light irradiation were studied.

2. Material and Methods

V_2O_5 nanoparticles were synthesized by vanadium acetylacetone ($VO(acac)_2$) and hexadecylamine ($CH_3(CH_2)_{15}NH_2$) as precursors. The solution mixture with the molar ratio of $VO(acac)_2$ and $CH_3(CH_2)_{15}NH_2$ = 2 : 1 was stirred for 1 h at 60°C. Then, it was heated at 90°C for 20 h. Finally, the nanoparticles were filtered and dried at oven.

Similar synthesis condition was used for the synthesis of V_2O_5 nanoflakes on PET fiber. In this work, a V_2O_5 seed layer was predeposited on the PET fiber to facilitate the growth of V_2O_5 nanostructures. The seed layer was deposited using a sol solution which contained of 0.015 mol of vanadium oxide and 30 wt% of hydrogen peroxide. The mixture was stirred for 1.5 h. Subsequently, the PET fiber which is precoated with 1 dodecanethiol was immersed into the sol solution for 15 min. Then, the fiber was dried in oven. This step was repeated for 3 times to ensure the V_2O_5 seed was uniformly coated on the fiber. Next, the fiber with V_2O_5 seed layer was immersed into the $VO(acac)_2$ and $CH_3(CH_2)_{15}NH_2$ solution for 20 h at 90°C for the growth of V_2O_5 nanoflakes.

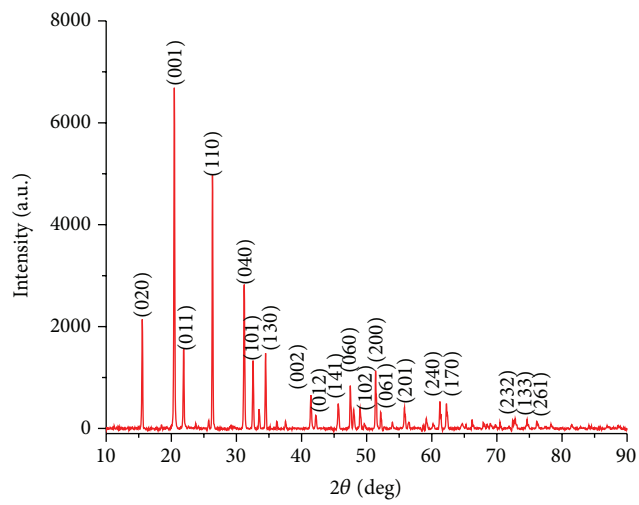

Figure 1: XRD pattern of V_2O_5 nanoparticles prepared by sol-gel method.

The morphologies of the nanostructures were examined using a Zeiss Supra 35 VP field emission scanning electron microscope (FESEM). The phase and crystallinity of the nanoparticles were characterized using a Philip PW 1729 X-ray diffractometer (Cu K_α, λ = 0.154 nm). The band gap of nanoparticles was determined by Perkin UV-Vis spectrometer. The effectiveness of V_2O_5 nanostructures to degrade 1.0×10^{-5} M of RhB solution under visible light was evaluated. A UV cutoff filter was used to remove any radiation below 400 nm and to ensure illumination by visible light only. The estimated V_2O_5 nanostructures used in this study were 15 mg. The degraded RhB solution was characterized by measuring the 553 nm absorption spectra of RhB using Cary 50 UV-Vis spectroscopy. In a separate experiment, isopropanol (IPA), which served as OH radical scavengers, was added into the RhB solution to study the role of OH radicals in this photocatalytic reaction.

3. Results and Discussion

3.1. V_2O_5 Nanoparticles and Their Photocatalytic Activity. The XRD pattern of the nanoparticles is shown in Figure 1. The XRD pattern could be indexed to V_2O_5 (JCPDS no. 60-0767). The diffraction peaks at 15.6°, 20.4°, 21.9°, 26.3°, 31.2°, 32.6°, 34.5°, 41.4°, 42.3°, 45.6°, 47.5°, 49.0°, 51.4°, 52.3°, 55.8°, 61.2°, and 62.3° corresponded to (020), (001), (011), (110), (040), (101), (130), (002), (012), (141), (060), (102), (200), (061), (201), (240), and (170) planes, respectively. No diffraction peaks for other elements were detected. The narrow and intense diffraction peaks reveal that the V_2O_5 nanoparticles were

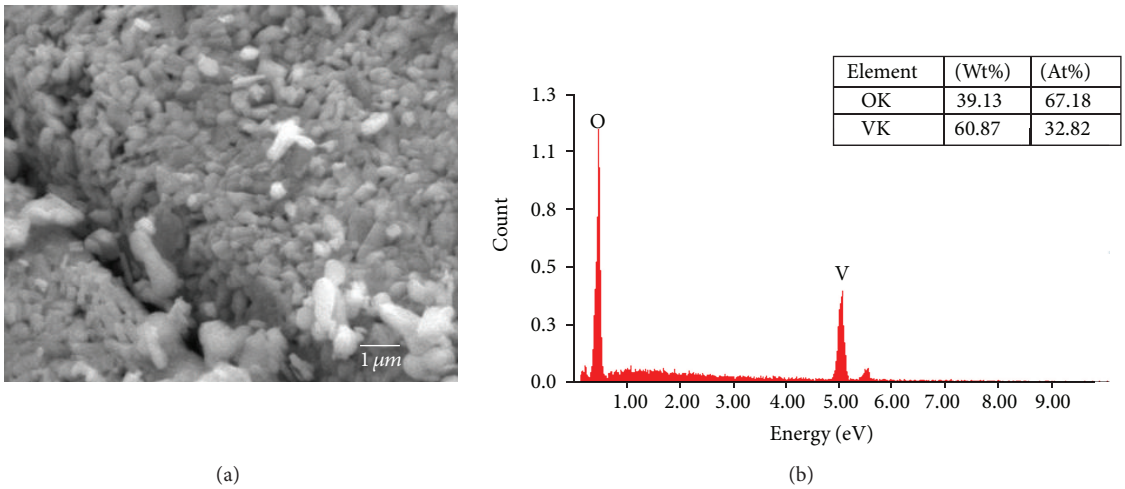

Figure 2: (a) SEM image and (b) EDX spectrum of V_2O_5 nanoparticles.

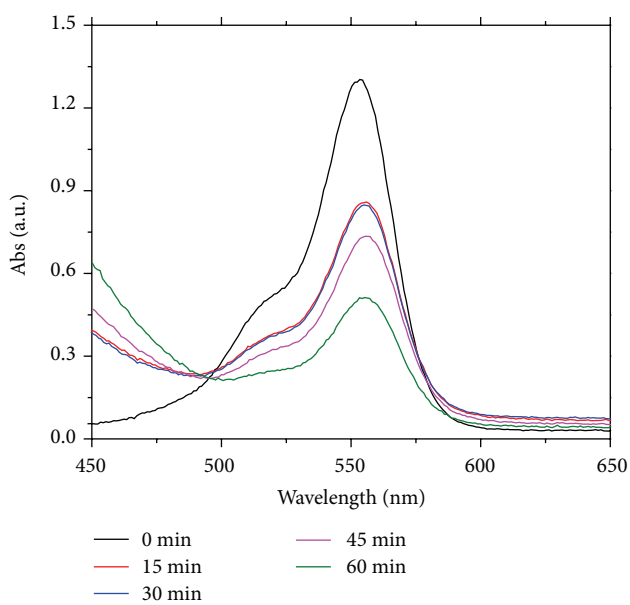

Figure 3: Absorbance spectra of RhB aqueous solution degraded by V_2O_5 nanoparticles under visible light irradiation.

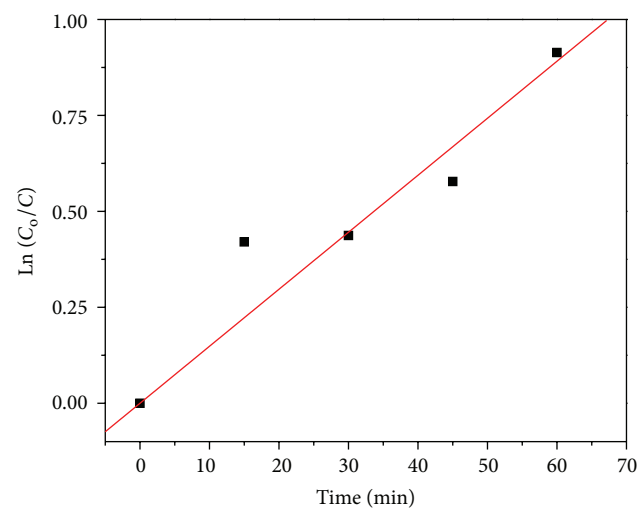

Figure 4: Photodegradation of RhB solution by V_2O_5 nanoparticles under visible light irradiation.

highly crystalline. The calculated size of V_2O_5 nanoparticles based on Scherrer equation was 53.5 nm. The morphology of V_2O_5 nanoparticles was determined by SEM image as shown in Figure 2(a). The V_2O_5 nanoparticles were rod-like with average length of 231.9 ± 14.9 nm. The EDX analysis as shown in Figure 2(b) indicates that there are no other impurity elements, besides V and O elements. The atomic percentage of V and O is 32.82% and 67.18%, respectively, which is close to the stoichiometric ratio of V_2O_5.

The effectiveness of V_2O_5 nanoparticles to degrade RhB solution under visible light was evaluated and is shown in Figure 3. The degraded RhB solution by V_2O_5 nanoparticles was characterized by measuring the 553 nm absorption spectra of RhB using Cary 50 UV-Vis spectroscopy. The intensity of the 553 nm absorption peak decreased as a function of irradiation time from 1.293 a.u. (initial absorbance) to 0.849 a.u. after 15 min and further decreased to 0.518 a.u. after 60 min. The decrease of this absorption peak was due to the breaking of the conjugated π-system in RhB chain by free radicals. This phenomenon is known as cycloreversion.

According to Lambert-beer law, the concentration of the solution (C) is proportional to the absorption spectrum (A). Thus, this allows the data to be replotted as a $\ln(C_o/C)$ versus irradiation time graph, as shown in Figure 4. The linear plot of $\ln(C_o/C)$ versus irradiation time indicates that degradation of RhB solution by V_2O_5 nanoparticles under visible light irradiation follows the first order kinetic. The rate constant of photodegradation of RhB by V_2O_5 nanoparticles under visible light irradiation, which could be determined from the slope of the graph, is 0.0149 min^{-1} (std. error = 0.0013 and R-square = 0.9611). This result suggests that V_2O_5 nanoparticles

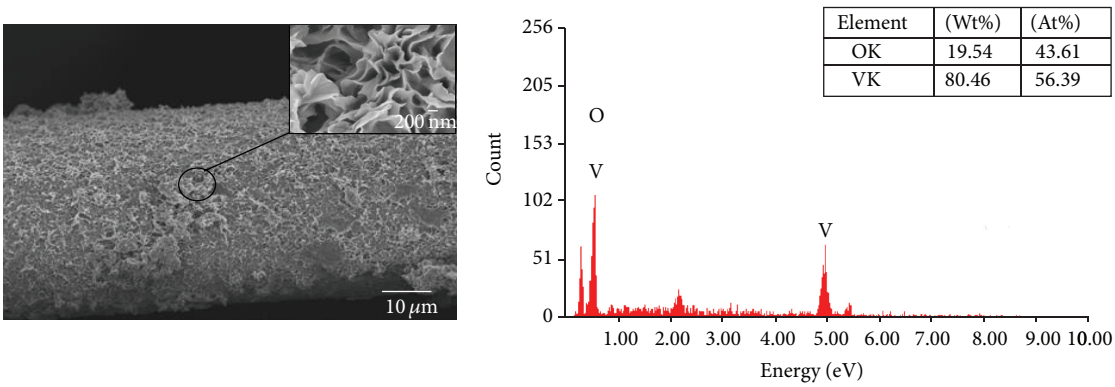

(a) (b)

Figure 5: (a) SEM images and (b) EDX spectrum of V_2O_5 nanoflakes grown on PET fiber.

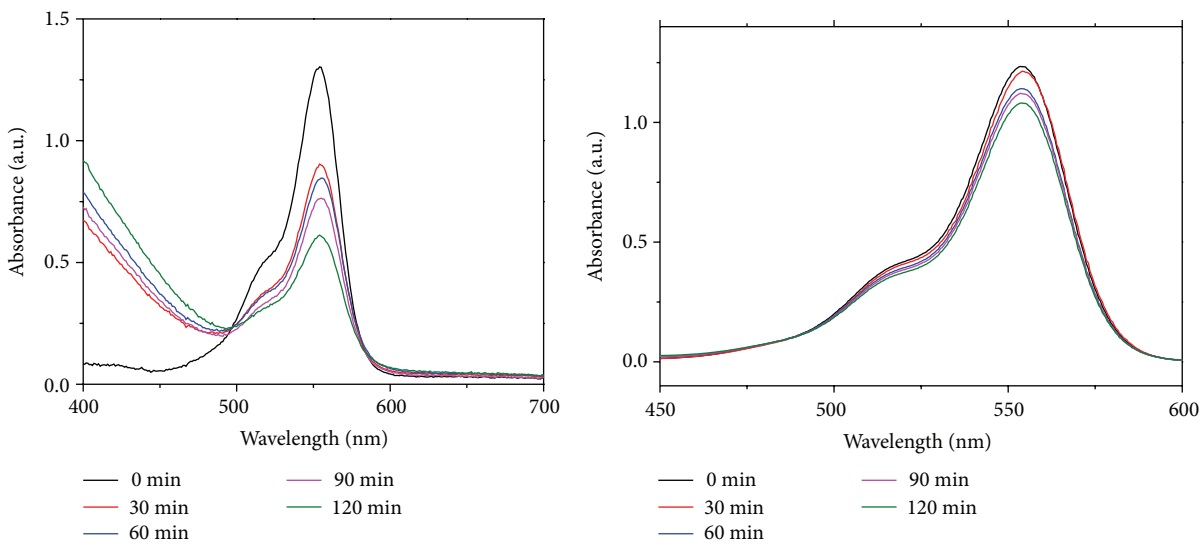

(a) (b)

Figure 6: Absorbance spectra of RhB aqueous solution (a) without and (b) with IPA degraded by V_2O_5 nanoflakes grown on PET fiber after visible light irradiation.

are visible-light-driven semiconductor photocatalysts. The photodegradation mechanism of RhB solution using V_2O_5 nanoparticles will be discussed in Section 3.3.

3.2. V_2O_5 Nanoflakes Grown on PET Fiber and Their Photocatalytic Activity. V_2O_5 nanoflakes were grown on PET fiber using the preestablished synthesis condition from Section 3.1. As shown in Figure 5(a), the PET fiber was fully covered by V_2O_5 nanoflakes. The thickness of the nanoflakes was in the range of 5–20 nm as shown in the inset of Figure 5(a). The EDX analysis in Figure 5(b) indicates that the main elements of the nanoflakes are V and O with the atomic percentage of 56.39% and 43.61%, respectively. No other impurity elements could be detected in the V_2O_5 nanoflakes.

The effectiveness of V_2O_5 nanoflakes grown on PET fiber to degrade RhB solution under visible light was evaluated. The color of RhB solution was faded gradually after being exposed to visible light as shown by the UV-Vis absorption spectrum of RhB solution in Figure 6(a). The intensity of the 553 nm absorbance peak of RhB decreased from 1.293 a.u. (initial absorbance) to 0.895 a.u. after 30 min irradiation. It is further reduced to 0.838 a.u. after 60 min and 0.608 a.u. after 120 min irradiation. The linear plot of $\ln(C_o/C)$ versus irradiation time in Figure 7(a) indicates that photodegradation of RhB by V_2O_5 nanoflakes under visible light irradiation follows the first order kinetic. The rate constant for V_2O_5 nanoflakes on PET fiber to degrade RhB solution under visible light irradiation is 0.0065 min^{-1} (std. error = 0.0006 and R-square = 0.9842). Although the rate constant of using V_2O_5 nanoflakes on PET fiber to degrade RhB solution under visible light is smaller than the rate constant using V_2O_5 nanoparticles, the result proved that the V_2O_5 nanoflakes could still degrade the RhB solution after growing on the PET fiber. Thus, the application of V_2O_5 nanoflakes grown on PET

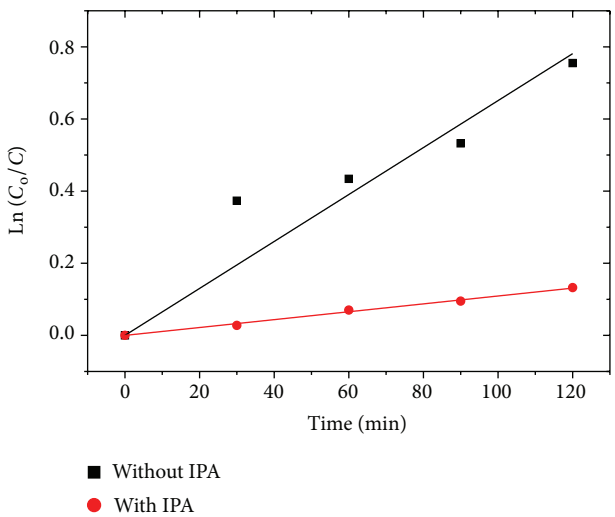

Figure 7: Photodegradation of RhB solution (a) without and (b) with IPA by V_2O_5 nanoflakes grown on PET fiber under visible light irradiation.

fiber to degrade organic pollutants in flowing water such as river is possible.

The photodegradation of RhB solution was deteriorated by V_2O_5 nanoflakes on PET fiber under visible light irradiation with the mixing of IPA as shown in Figures 6(b) and 7(b). The rate constant of the reaction with IPA is 0.0011 min^{-1} (std. error = 0.0002 and R-square = 0.999). As IPA is known as an OH free radical scavenger [26, 27], the significant decrease of rate constant indicates that the photodegradation of RhB solution was dominant by the OH free radicals that were generated by V_2O_5 nanoflakes on PET fiber under visible light irradiation.

3.3. Photodegradation Mechanism of RhB Solution by V_2O_5 under Visible Light Irradiation. The photodegradation of RhB solution by V_2O_5 could be explained by adsorption-oxidation-desorption mechanism. The optical band gap of V_2O_5 nanoparticles measured by UV-Vis spectrometer is 2.41 eV as indicated in Figure 8. The E_v and E_c of V_2O_5 nanoparticles in NHE are 0.40 eV and 2.81 eV, respectively, as shown in Figure 9. This result is in good agreement with the reported values by Miyauchi et al. and Viswanathan [21, 28]. As illustrated in Figure 9, the band edge of conduction band (E_c) of V_2O_5 nanoparticles is more positive to the absolute electronegativity of oxygen (−0.046 eV). Thus, the excited electrons (e^-_{cb}) in the conduction band do not favor for the reduction of oxygen molecules into $O_2^{\bullet}$ free radicals. However, the band edge of valence band (E_v) (2.81 eV) is more positive than the oxidation potential of water (1.99 eV). In this case, the holes (h^+_{vb}) are able to produce $OH^{\bullet}$ free radicals [29–31]. These free radicals are responsible for the degradation of RhB dye into less harmful byproduct such as water as shown in (1)–(3). Generally, V_2O_5 nanoparticles and nanoflakes took a longer time to decolorize the RhB solution as compared to ZnO [6–10] and TiO_2 [11–13]. The slower photodegradation efficiency was likely attributed to

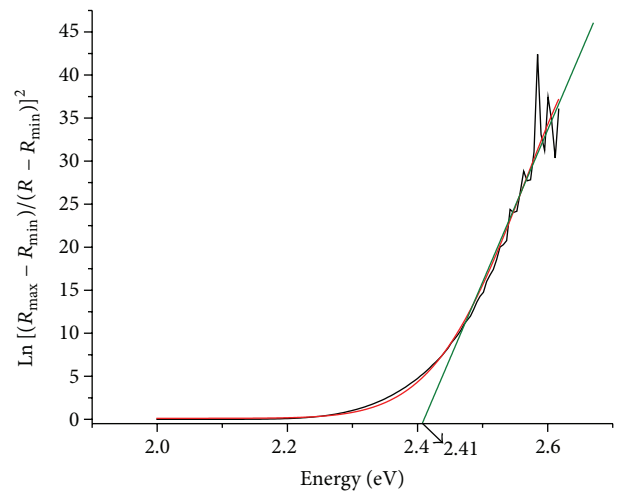

Figure 8: The band gap of V_2O_5 nanoparticles.

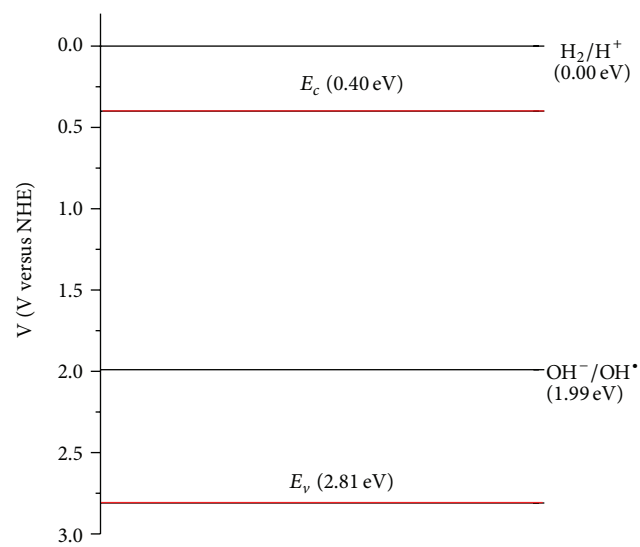

Figure 9: The band structure model of V_2O_5.

the limited number of free radicals produced by V_2O_5 as only the photogenerated holes were able to produce free radicals. Consider the following:

$$V_2O_5 + h\nu \longrightarrow h^+_{vb} + e^-_{cb} \quad (1)$$

$$h^+_{vb} + H_2O \longrightarrow H^+ + OH^{\bullet} \quad (2)$$

$$\text{RhB dye} + O_2^{\bullet -} + OH^{\bullet} \longrightarrow \text{byproducts} \quad (3)$$

4. Conclusions

V_2O_5 nanoparticles and V_2O_5 nanoflakes on fiber were successfully synthesized via sol-gel method. The V_2O_5 nanoparticles were rod-like with average length of 231.9 ± 14.9 nm, whereas the thickness of the nanoflakes was in the range of 5–20 nm. The photocatalytic activities for both V_2O_5 nanoparticles and V_2O_5 nanoflakes grown on fiber were

$0.0149\,\text{min}^{-1}$ and $0.0065\,\text{min}^{-1}$, respectively, under visible light irradiation. These results indicate that both V_2O_5 nanostructures could be used as visible-light-driven photocatalysts to remove organic pollutants. The slow photodegradation rate of V_2O_5 nanostructures to degrade RhB dye under visible light irradiation is proposed due to the slow free radicals ($OH^{\bullet}$) generation rate as only the photogenerated holes are positively enough to produce $OH^{\bullet}$ based on the energy diagram.

Conflict of Interests

The authors declare that there is no conflict of interests regarding the publication of this paper.

Acknowledgments

The authors would like to acknowledge the USM Postgraduate Research Grant Scheme (PRGS) (1001/PBAHAN/8036010) and the USM Research University Grant (RU) (1001/PBAHAN/814200) for the financial support to conduct this project.

References

[1] B. Neppolian, H. C. Choi, S. Sakthivel, B. Arabindoo, and V. Murugesan, "Solar/UV-induced photocatalytic degradation of three commercial textile dyes," *Journal of Hazardous Materials*, vol. 89, no. 2-3, pp. 303–317, 2002.

[2] G. S. Gupta, G. Prasad, and V. N. Singh, "Removal of chrome dye from aqueous solutions by mixed adsorbents: fly ash and coal," *Water Research*, vol. 24, no. 1, pp. 45–50, 1990.

[3] A. Rozzi, M. Antonelli, and M. Arcari, "Membrane treatment of secondary textile effluents for direct reuse," *Water Science and Technology*, vol. 40, no. 4-5, pp. 409–416, 1999.

[4] L. Xu, W. Li, S. Lu, Z. Wang, Q. Zhu, and Y. Ling, "Treating dyeing waste water by ceramic membrane in crossflow microfiltration," *Desalination*, vol. 149, no. 1–3, pp. 199–203, 2002.

[5] J. Mo, J. Hwang, J. Jegal, and J. Kim, "Pretreatment of a dyeing wastewater using chemical coagulants," *Dyes and Pigments*, vol. 72, no. 2, pp. 240–245, 2007.

[6] N. Daneshvar, S. Aber, M. S. Seyed Dorraji, A. R. Khataee, and M. H. Rasoulifard, "Preparation and investigation of photocatalytic properties of ZnO nanocrystals: effect of operational parameters and kinetic study," *World Academy of Science Engineering and Technology*, vol. 29, pp. 267–272, 2007.

[7] R. Y. Hong, J. H. Li, L. L. Chen et al., "Synthesis, surface modification and photocatalytic property of ZnO nanoparticles," *Powder Technology*, vol. 189, no. 3, pp. 426–432, 2009.

[8] J. Xie, Y. Li, W. Zhao, L. Bian, and Y. Wei, "Simple fabrication and photocatalytic activity of ZnO particles with different morphologies," *Powder Technology*, vol. 207, no. 1–3, pp. 140–144, 2011.

[9] S. N. Q. A. Abd Aziz, S. Y. Pung, N. N. Ramli, and Z. Lockman, "Growth of ZnO nanorods on stainless steel wire using chemical vapour deposition and their photocatalytic activity," *The Scientific World Journal*, vol. 2014, Article ID 252851, 9 pages, 2014.

[10] Y. L. Chan, S. Y. Pung, and S. Sreekantan, "Degradation of organic dye using ZnO nanorods based continuous flow water purifier," *Journal of Sol-Gel Science and Technology*, vol. 66, no. 3, pp. 399–405, 2013.

[11] T. G. Smijs and S. Pavel, "Titanium dioxide and zinc oxide nanoparticles in sunscreens: Focus on their safety and effectiveness," *Nanotechnology, Science and Applications*, vol. 4, no. 1, pp. 95–112, 2011.

[12] H. A. Bullen and S. J. Garrett, *TiO_2 Nanoparticles for Photocatalysis*, Michigan State University, East Lansing, Mich, USA, 2003.

[13] H. Esfahani, A. H. Javadi, M. A. Farahmandnejad, P. Nourpour, and K. Shabani, "Study on kinetic of UV and solar assisted photocatalytic degradation of rhodamine B by TiO_2 nanostructure layer," *Materials Technology*, vol. 27, no. 3, pp. 261–266, 2012.

[14] R. Mohan, K. Krishnamoorthy, and S. Kim, "Enhanced photocatalytic activity of Cu-doped ZnO nanorods," *Solid State Communications*, vol. 152, no. 5, pp. 375–380, 2012.

[15] D. Zhang and F. Zeng, "Visible light-activated cadmium-doped ZnO nanostructured photocatalyst for the treatment of methylene blue dye," *Journal of Materials Science*, vol. 47, no. 5, pp. 2155–2161, 2012.

[16] J. H. Cheng, G. Shao, H. J. Yu, and J. J. Xu, "Excellent catalytic and electrochemical properties of the mesoporous MnO_2 nanospheres/nanosheets," *Journal of Alloys and Compounds*, vol. 505, no. 1, pp. 163–167, 2010.

[17] J. Ge and J. Qu, "Degradation of azo dye acid red B on manganese dioxide in the absence and presence of ultrasonic irradiation," *Journal of Hazardous Materials*, vol. 100, no. 1–3, pp. 197–207, 2003.

[18] Y. Wang, Z. Zhang, Y. Zhu et al., "Nanostructured VO_2 photocatalysts for hydrogen production," *ACS Nano*, vol. 2, no. 7, pp. 1492–1496, 2008.

[19] S. R. Segal, S. L. Suib, X. Tang, and S. Satyapal, "Photoassisted decomposition of dimethyl methylphosphonate over amorphous manganese oxide catalysts," *Chemistry of Materials*, vol. 11, no. 7, pp. 1687–1695, 1999.

[20] F. D. Mai, C. C. Chen, J. L. Chen, and S. C. Liu, "Photodegradation of methyl green using visible irradiation in ZnO suspensions: determination of the reaction pathway and identification of intermediates by a high-performance liquid chromatography-photodiode array-electrospray ionization-mass spectrometry method," *Journal of Chromatography A*, vol. 1189, no. 1-2, pp. 355–365, 2008.

[21] M. Miyauchi, A. Nakajima, T. Watanabe, and K. Hashimoto, "Photocatalysis and photoinduced hydrophilicity of various metal oxide thin films," *Chemistry of Materials*, vol. 14, no. 6, pp. 2812–2816, 2002.

[22] J. Wei and J. Zhang, "Hydrothermal synthesis and characterization of vanadium oxide nanotubes," *Advanced Materials Research*, vol. 11-12, pp. 535–538, 2006.

[23] H. Yin, K. Yu, H. Peng et al., "Porous V_2O_5 micro/nano-tubes: synthesis via a CVD route, single-tube-based humidity sensor and improved Li-ion storage properties," *Journal of Materials Chemistry*, vol. 22, no. 11, pp. 5013–5019, 2012.

[24] T. Blanquart, J. Niinistö, M. Gavagnin et al., "Atomic layer deposition and characterization of vanadium oxide thin films," *RSC Advances*, vol. 3, no. 4, pp. 1179–1185, 2013.

[25] M. Gotić, S. Popović, M. Ivanda, and S. Musić, "Sol-gel synthesis and characterization of V_2O_5 powders," *Materials Letters*, vol. 57, no. 21, pp. 3186–3192, 2003.

[26] N. Serpone, D. Lawless, R. Khairutdinov, and E. Pelizzetti, "Subnanosecond relaxation dynamics in TiO_2 colloidal sols (particle sizes R_p = 1.0–13.4 nm). Relevance to heterogeneous photocatalysis," *Journal of Physical Chemistry*, vol. 99, no. 45, pp. 16655–16661, 1995.

[27] R. A. Palominos, M. A. Mondaca, A. Giraldo, G. Peñuela, M. Pérez-Moya, and H. D. Mansilla, "Photocatalytic oxidation of the antibiotic tetracycline on TiO_2 and ZnO suspensions," *Catalysis Today*, vol. 144, no. 1-2, pp. 100–105, 2009.

[28] B. Viswanathan, *Photo-Electrochemical Processes—Principles and Possibilities*, National Centre for Catalysis Research Indian Institute of Technology Madras, Chennai, India, 2011.

[29] B. Pan, Y. Xie, S. Zhang, L. Lv, and W. Zhang, "Visible light photocatalytic degradation of RhB by polymer-CdS nanocomposites: role of the host functional groups," *ACS Applied Materials and Interfaces*, vol. 4, no. 8, pp. 3938–3943, 2012.

[30] W. K. Burton, N. Cabrera, and F. C. Frank, "The growth of crystals and the equilibrium structure of their surfaces," *The Philosophical Transactions of the Royal Society A*, vol. 243, pp. 299–358, 1951.

[31] J. Fu, Y. Tian, B. Chang, F. Xi, and X. Dong, "BiOBr-carbon nitride heterojunctions: synthesis, enhanced activity and photocatalytic mechanism," *Journal of Materials Chemistry*, vol. 22, no. 39, pp. 21159–21166, 2012.

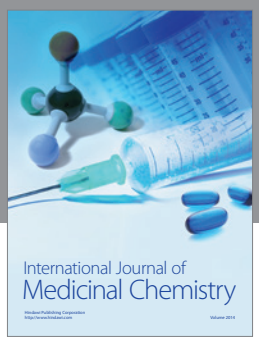

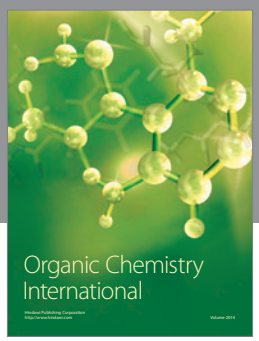

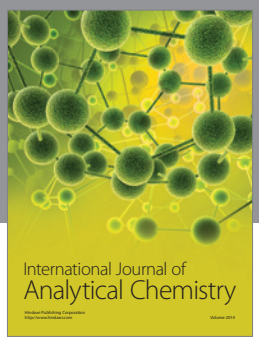

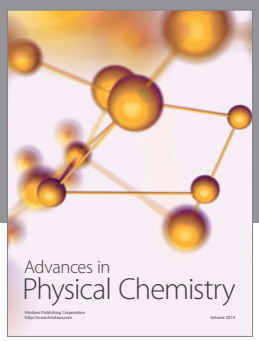

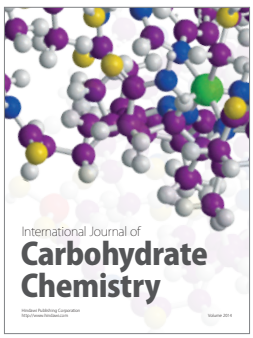

Hindawi

Submit your manuscripts at
http://www.hindawi.com